Calcium Release in Frog Cut Twitch Fibers Exposed to Different Ionic Environments under Voltage Clamp

Chiu Shuen Hui
Department of Physiology and Biophysics, Indiana University Medical Center, Indianapolis, Indiana 46202

ABSTRACT Calcium release was measured in highly stretched frog cut twitch fibers mounted in a double Vaseline-gap voltage clamp chamber, with the internal solution containing 20 mM EGTA plus 0.4 or 1.8 mM added calcium. Rise in myoplasmic [Ca^{2+}] was monitored with antipyrylazo III as the indicator at a temperature of 13 to 14°C. The waveform of calcium release rate (Rel) computed from the absorbance change showed an early peak (Rel_p) followed by a maintained phase (Rel_m). Each Rel_p-versus-V plot was fitted with a Boltzmann distribution function. The maximum value of Rel_p ($Rel_{p,max}$) was compared in various calcium-containing external solutions. The average value in a Cl^- solution was about one-third larger than those in a $CH_3SO_3^-$ or gluconate solution, whereas the values in the $CH_3SO_3^-$ and gluconate solutions had no statistically significant difference. In external solutions containing $CH_3SO_3^-$ or gluconate, a replacement of the Ca^{2+} with Mg^{2+} reduced $Rel_{p,max}$ by 30 to 50%, on average. The values of $Rel_{p,max}$ also had no statistically significant difference among calcium-free external solutions containing different impermeant anions. An increase of the nominal free [Ca^{2+}] in the end-pool solution from a reduced to the normal physiological level increased the value of $Rel_{p,max}$, and also slowed the decay of the maintained phase of the Rel waveform. The Rel waveforms in the Cl^- and $CH_3SO_3^-$ solutions were compared in the same fiber at a fixed potential. $CH_3SO_3^-$ increased the time to peak, reduced Rel_p, and increased Rel_m, and the effects were partially reversible. Under the hypothesis that the decay of the peak was due to calcium inactivation of calcium release, the inactivation was larger in Cl^- than in $CH_3SO_3^-$, in qualitative agreement with the ratio of Rel_p in the two solutions. Under the alternative hypothesis that the peak and the maintained phase were separately gated by calcium and depolarization, respectively, then $CH_3SO_3^-$ appeared to decrease the calcium-gated component and increase the voltage-gated component.

INTRODUCTION

Intracellular calcium release from the sarcoplasmic reticulum (SR) in skeletal muscle has been studied intensively with the help of the metallochromic indicators, such as arsenazo III, antipyrylazo III (ApIII), and purpurate-3,3′diacetic acid (PDAA), in intact fibers (Miledi et al., 1977; Baylor et al., 1982a,b,c, 1983a,b; Konishi and Baylor, 1991) and in cut fibers (Kovacs et al., 1979, 1983; Palade and Vergara, 1982; Melzer et al., 1986; Maylie et al., 1987a,b,c; Schneider et al., 1987; Schneider and Simon, 1988; Hirota et al., 1989; Maylie and Hui, 1991). When the calcium transients were elicited by action potentials, a normal Ringer solution containing Cl^- as the major anion was used as the external solution. When the calcium transients were elicited by voltage-clamped pulses, the Cl^- in the external solution was replaced with an impermeant anion, such as sulphate, methanesulphonate, or gluconate, to abolish the anionic current through the outer membranes. This substitution had some influence on charge movement. Specifically, when charge movement was measured in voltage-clamped cut fibers exposed to an internal solution containing 20 mM EGTA without added calcium and an external solution containing Cl^- as the major anion, the charge movement transient, upon depolarization, showed an early I_β component followed by a prominent I_γ hump component (Hui and Chandler, 1990). Replacement of the Cl^- with an impermeant anion had very little effect on I_γ. In contrast, I_β was increased by sulphate (Hui and Chandler, 1990), unaffected by methanesulphonate (Hui, 1991), and suppressed by gluconate (Hui and Chen, 1995). Thus, anion substitution can potentially provide useful information about the individual roles of the two components of charge movement in triggering calcium release.

The first aim of this paper is to answer the question whether the choice of the major anion in the external solution makes any difference in the rate of calcium release. If the charge associated with I_γ, i.e., Q_γ, is the trigger for calcium release, as suggested by Huang (1982), Hui (1983a,b), and Vergara and Caputo (1983), then a replacement of the Cl^- with an impermeant anion in the external solution is not expected to have a noticeable effect on calcium release. On the other hand, if Q_β is involved in triggering calcium release, then the rate of calcium release should be different when a different anion is present in the external solution. An alternative hypothesis can be proposed for a possible effect of external anions on calcium release. Coronado and associates (Sukhareva et al., 1994; Patel et al., 1996) reported that Cl^- increases calcium release in SR vesicles and lipid bilayers. If sufficient Cl^- is present in the myoplasm, it might enhance calcium release in live fibers to some extent, although not necessarily as much as that observed in SR vesicles and lipid bilayers, because the [Cl^-] was much higher in those preparations.

Received for publication 8 April 1999 and in final form 17 May 1999.

Address reprint requests to Dr. Chiu Shuen Hui, Department of Physiology and Biophysics, Indiana University Medical Center, 635 Barnhill Drive, Indianapolis, IN 46202. Tel.: 317-274-8238; Fax: 317-274-3318; E-mail: cshui@iupui.edu.

0006-3495/99/10/2123/14 $2.00

It will be shown in this paper that the choice of external anion affects the rate of calcium release, but the variation does not match the pattern of variation of Q_β or the lack of variation of Q_γ just described. This discrepancy will be explained by arguing that the two groups of experiments studying charge movement or calcium release separately were not performed under identical experimental conditions. Nonetheless, the results are in qualitative agreement with the observations in SR vesicles and lipid bilayers. In addition, they alert us that the impermeant anions attenuate the normal calcium release measured with the physiological anion Cl^-.

The second aim of this paper is to investigate the effects of extracellular and myoplasmic Ca^{2+} on calcium release rate. In skeletal muscle, the sole supply of Ca^{2+} for contractile activation is from the SR, as fibers bathed in a calcium-free external solution could contract repetitively (Armstrong et al., 1972). In the study of excitation-contraction coupling in skeletal muscle, calcium-free external solutions are often used to avoid the appearance of the L-type calcium current whenever long depolarizing pulses are used, but whether the absence of extracellular Ca^{2+} affects intracellular calcium release remains an open question. On the other hand, myoplasmic Ca^{2+} directly affects the reloading of the SR and should have a more direct influence on the calcium transient than extracellular Ca^{2+}. Relevant to this, a high concentration (10–20 mM) of intracellular EGTA has been used successfully by various investigators to suppress movement artifact in cut fibers. The EGTA is expected to attenuate the calcium transient because it chelates the myoplasmic Ca^2. To what extent will this low, or even intermediate, $[Ca^{2+}]_i$ affect the calcium release rate is of fundamental interest to muscle physiologists.

The last aim of this paper is to gain some knowledge about the differential responses of the early peak and the maintained phase of calcium release under voltage clamp to a change in the external anion. Two hypotheses have been proposed to explain the existence of the two phases. In one hypothesis, the decay from the peak rate to the maintained rate is attributed to the inactivation of calcium release by the released Ca^{2+} (Baylor et al., 1983a; Schneider and Simon, 1988; Simon et al., 1991; Hollingworth et al., 1992; Jong et al., 1993, 1995; Pape et al., 1998). This negative feedback mechanism is called calcium inactivation of calcium release, which was also observed in the cardiac preparation (Fabiato, 1985). In another hypothesis, the peak and the maintained phase of the waveform are viewed as two distinct components: the maintained component is gated by depolarization, whereas the peak component is triggered by the released Ca^{2+} (Jacquemond et al., 1991; Rios and Pizarro, 1995). The latter positive feedback mechanism is called calcium-induced calcium release, which was first discovered by Endo et al. (1970) and Ford and Podolsky (1970). Although no definite conclusion can be drawn to support or reject either hypothesis, the results obtained provide some insight into the likelihood of either hypothesis.

A preliminary report of some of the findings has been published previously (Hui, 1997).

METHODS

Muscle and fiber preparation

All experiments were performed on cut twitch fibers from English frogs, *Rana temporaria*, cold acclimated in a refrigerator at around 4°C. Animals were killed by decapitation and destruction of the brain and spinal cord. Cut fibers were dissected from semitendinosus muscles and mounted in a double Vaseline-gap chamber with a procedure similar to that used by Kovacs et al. (1983) and Irving et al. (1987). ApIII was used as the calcium indicator in all experiments. To facilitate the entry of ApIII into the myoplasm, the outer membranes of the fiber in the end pools were permeabilized by a 2-min exposure to 0.01% saponin (Sigma Chemical Co., St. Louis, MO). The beginning of the treatment marked time 0 of an experiment. Both end pools were rinsed with solution A, and then filled with an internal solution (solution B, C, or D). Finally, the solution in the center pool was changed to an external solution (one of solutions E-I).

The chamber was mounted on the microscope stage during the 20th to 23rd minute. The voltage clamp was turned on and the fiber was repolarized. Temperature was controlled at 13–14°C by a Peltier cooling device (Midland-Ross Corp., Cambridge, MA). A 30-min equilibration period was allowed for the fiber to recover from the prolonged depolarization during its exposure to the relaxing solution and for various ions to diffuse into the myoplasm in the center pool region. Subsequent solution changes were carried out with the fiber under voltage clamp.

Composition of solutions

The compositions of the relaxing, internal, and external solutions are given in Table 1. Cs^+ in internal solutions B-D and TEA^+ and Rb^+/Cs^+ in external solutions E-I were used to suppress K^+ currents. Tetrodotoxin (Calbiochem-Novabiochem International, La Jolla, CA) in external solutions was used to block Na^+ current. TEA-Cl and $(TEA)_2SO_4$ were bought from R.S.A. Corp. (Ardsley, NY). TEA-methanesulphonate (TEA-CH_3SO_3) and TEA-gluconate were prepared by titrating, respectively, methanesulphonic acid (Aldrich Chemical Co., Milwaukee, WI) and gluconic acid lactone (Sigma) with TEA-OH (R.S.A.). Cs_2-creatine phosphate was prepared from Na_2-creatine phosphate (Calbiochem-Novabiochem) by ion exchange. Special care was taken to minimize the contaminating Ca^{2+} in the prepared stock solution. With 20 mM EGTA, the free $[Ca^{2+}]$ in the internal solution was estimated to be $<10^{-12}$ M. In the presence of 0.4 mM added calcium in solution C (or 1.8 mM added calcium in solutions B and D), the free $[Ca^{2+}]$ was estimated to be ~10 (or ~50) nM, which is less than (or close to) the physiological level.

Voltage clamp and data acquisition

The instrumentation for data acquisition was similar to that used by Irving et al. (1987) and upgraded to facilitate the inclusion of more input channels and the digitization of a larger array of points in each channel (Pape et al., 1995). The new data acquisition module was designed and fabricated by the Biomedical Instrumentation Laboratory of the Yale University Department of Cellular and Molecular Physiology (New Haven, CT). Ten analog signals, including six optical signals (see below), three electrical signals V_1, V_2, and I_2, and the temperature signal, were connected to the input channels of the module. The cutoff frequency of the eight-pole Bessel filter in each channel was set at 0.6 kHz. Data were digitized at a rate of 100 kHz and sent to a PDP 11/73 computer (Qualogy, San Jose, CA) for processing. The points in each channel were compressed before storage. As a result, each point in a stored trace corresponds to 1 ms.

Holding potential was set at −90 mV. Control pulses were applied from −110 mV to the holding potential and test pulses from the holding potential to the potentials desired. Throughout an experiment, the condition

TABLE 1 Composition of solutions used in experiments

Relaxing solution									
Solution	Potassium glutamate		$MgSO_4$		K_2-EGTA				K_2-Pipes
A	120		1		0.1				5
End-pool or internal solutions									
Solution	Cesium glutamate	Cs_2-CP	$MgSO_4$	Cs_2-EGTA	Cs_2-ATP	Cs_2-PEP	Mg-ATP	Cs-Mops	Total Ca
B	42.5	20	0	20	0	0	5.5	20	1.8
C	50	20	6.8	20	5.5	5	0	5	0.4
D	50	20	6.8	20	5.5	5	0	5	1.8
Center-pool or external solutions											
Solution	TEA-Cl	TEA-CH_3SO_3	$(TEA)_2SO_4$	TEA-gluc	RbCl	Cs_2SO_4	$CaCl_2$	$Ca(CH_3SO_3)_2$	$Ca(gluc)_2$	$Mg(CH_3SO_3)_2$	$MgSO_4$
E	120	—	—	—	2.5	—	1.8	—	—	—	—
F	—	115	—	—	—	5	—	2	—	—	—
G	—	100	—	—	—	5	—	—	—	10	—
H	—	—	75	—	—	5	—	—	—	—	10
I	—	—	—	117	—	5	—	—	10	—	—

All concentrations are in mM. Pipes, piperazine-N,N′-bis[2-ethane sulphonic acid; CP, creatine phosphate; PEP, phospho(enol)pyruvate; Mops, 3-(N-morpholino) propanesulphonic acid; TEA, tetraethylammonium; CH_3SO_3, methanesulphonate; gluc, gluconate. Solutions B through D contained 5 mM glucose. Solutions E through I contained 1 μM tetrodotoxin and 5 mM Mops. The relaxing and internal solutions were titrated to pH 7.0 with KOH and CsOH, respectively. The external solutions were titrated to pH 7.1 with TEA-OH.

of the fiber was tracked by monitoring the holding current and fiber diameter. Subsequent data analysis included linear cable analysis of the control records, which yielded information about myoplasmic resistance (r_i), membrane resistance (r_m), membrane capacitance (c_m), and gap factor of the Vaseline seals defined by $r_e/(r_e + r_i)$ (Chandler and Hui, 1990), in which r_e represents the external resistance underneath the Vaseline seals.

Optical measurement

The experimental procedure and processing of the optical records followed those of Irving et al. (1987) and Maylie et al. (1987a,b) and had been used in our optical experiments (Maylie and Hui, 1991). The optical system was built on an upright microscope (model ACM, Carl Zeiss, New York, NY). Optical measurements were made with a 55.5-μm diameter spot of light focused on the axis of the fiber segment located in the center pool. Because three wavelengths are required to accurately describe the calcium indicator signal in muscle (Baylor et al., 1982a), the transmitted light was separated into three beams with two beam-splitting cubes. The beams were made quasi-monochromatic by passing through three interference filters with peak transmission wavelengths at 550 nm (10 nm bandwidth), 720 nm (30 nm) and 810 nm (30 nm). Each beam was further split into two beams of linear polarizations (0 and 90° with respect to the fiber axis) with a polarizing beam-splitting cube.

The intensities of the six resulting beams were monitored with photodiodes (model UV-100B, EG&G Electro-Optics Division, Salem, MA) and fed to the inputs of the optical channels of the data acquisition module. The absorbance at each wavelength A (λ) was computed from the 1:2 average of A_0:A_{90} (mode 1 in Irving et al., 1987). The intrinsic absorbance signal $\Delta A_i(810)$ was filtered by a 0.05-kHz digital Gaussian filter (Colquhoun and Sigworth, 1983). The procedures described in Maylie et al. (1987a) were used to subtract the contributions due to the intrinsic absorbance changes to yield the dye-related $\Delta A(720)$.

Computation of calcium release rate

In this article, the term "calcium release rate" (Rel) refers to the $d\Delta[Ca_T]/dt$ signal, in which Ca_T represents the total amount of calcium (free and bound) in the myoplasm. Rel was computed from the dye-related $\Delta A(720)$, based on a model similar to the one used by Baylor et al. (1983a), but modified to include the binding of Ca^{2+} to EGTA in addition to its binding to ApIII, troponin, and parvalbumin. The values of the parameters used in the modeling were adopted from Maylie et al. (1987b), who also provided references for the sources of some of the values. They were: 1.46×10^4 M^{-1} cm^{-1} for $\Delta\epsilon$ (720) of the Ca^{2+}-ApIII complexes, 3.4×10^{-8} M^2 for the apparent k_D between Ca^{2+} and ApIII, 240 μM for the total concentration of troponin, 0.575×10^8 $M^{-1}s^{-1}$ and 115 s^{-1} for k_1 and k_{-1} of Ca^{2+} binding to troponin, 2 mM for the total concentration of parvalbumin, 1.25×10^8 $M^{-1}s^{-1}$ and 0.5 s^{-1} for k_1 and k_{-1} of Ca^{2+} binding to parvalbumin, 3.3×10^4 $M^{-1}s^{-1}$ and 3.0 s^{-1} for k_1 and k_{-1} of Mg^{2+} binding to parvalbumin, 1.0×10^6 $M^{-1}s^{-1}$ and 0.5 s^{-1} for k_1 and k_{-1} of Ca^{2+} binding to EGTA. Only the computed Rel, but not the absorbance, traces will be shown throughout this article, except in Fig. 1. The peak amplitude of Rel, represented by Rel_p, and the time-to-peak in each trace were determined by fitting the peak with a parabolic function.

RESULTS

Voltage dependence of calcium release in a TEA-Cl external solution

The first group of experiments studying the voltage dependence of calcium release were performed on cut fibers bathed in an external solution containing the physiological anion Cl^-. Results from a typical experiment are shown in Figs. 1 and 2. Calcium release was elicited by a sequence of test pulses in a monotonically increasing order of amplitude. The pulses were applied once every 3 min to allow time for reloading the SR with Ca^{2+}.

Fig. 1 *A* shows the dye-related ΔA_{720} traces that were computed from the raw ΔA_{720} signals with the procedure developed by Maylie et al. (1987a). For potentials < -20 mV, the pulse durations were 150 to 400 ms, but only the

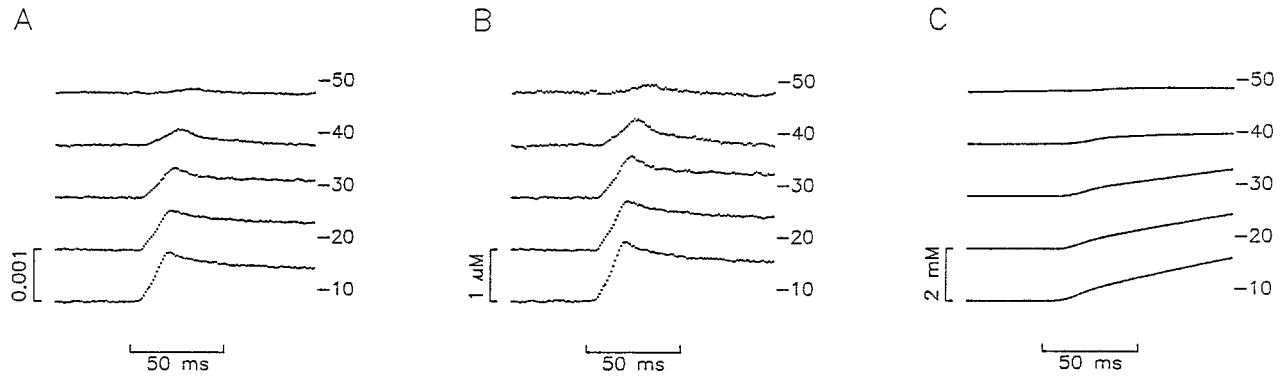

FIGURE 1 Computation of calcium release in a cut fiber bathed in a TEA-Cl solution. The end pools contained solution D and the center pool contained solution E. From the beginning to the end of the experiment, the holding current changed from −37 to −53 nA and $r_e/(r_e + r_i)$ decreased from 0.983 to 0.976. At the 62nd minute, 0.73 mM ApIII was added to the end pools. At the 127th minute, the [ApIII] in the end pools was reduced to 0.22 mM. Representative traces were taken from the 137th to the 170th minute, during which the myoplasmic [ApIII] increased from 0.37 to 0.54 mM. (*A*) Dye-related ΔA_{720} traces. (*B*) ΔFree $[Ca^{2+}]$ traces. (*C*) $\Delta[Ca_T]$ traces. Fiber diameter = 107 μm; sarcomere length = 4 μm. The numbers to the right of the traces show the potentials during the test pulses. The left tick of each horizontal scale bar marks the rising edge of the voltage pulse; the same alignment also holds in the following figures.

first 100 ms of the signals are shown, because the early part of calcium release is the focus of this article. The later part of the release was not analyzed for the reason given below. The traces in Fig. 1 *B* show the Δfree $[Ca^{2+}]$ waveforms at the various potentials. These traces were computed from the traces in Fig. 1 *A* using the assumed values given in Methods for the extinction coefficient of the Ca^{2+}-ApIII complex and the apparent k_D between Ca^{2+} and ApIII, together with the measured myoplasmic [ApIII] at the instant the raw traces were taken. The traces in Fig. 1 *C* show the $\Delta[Ca_T]$ waveforms at the various potentials. These were obtained by numerically solving a system of simultaneous differential equations (similar to the model developed by Baylor et al., 1983a) that describe the binding of Ca^{2+} to arsenazo III,

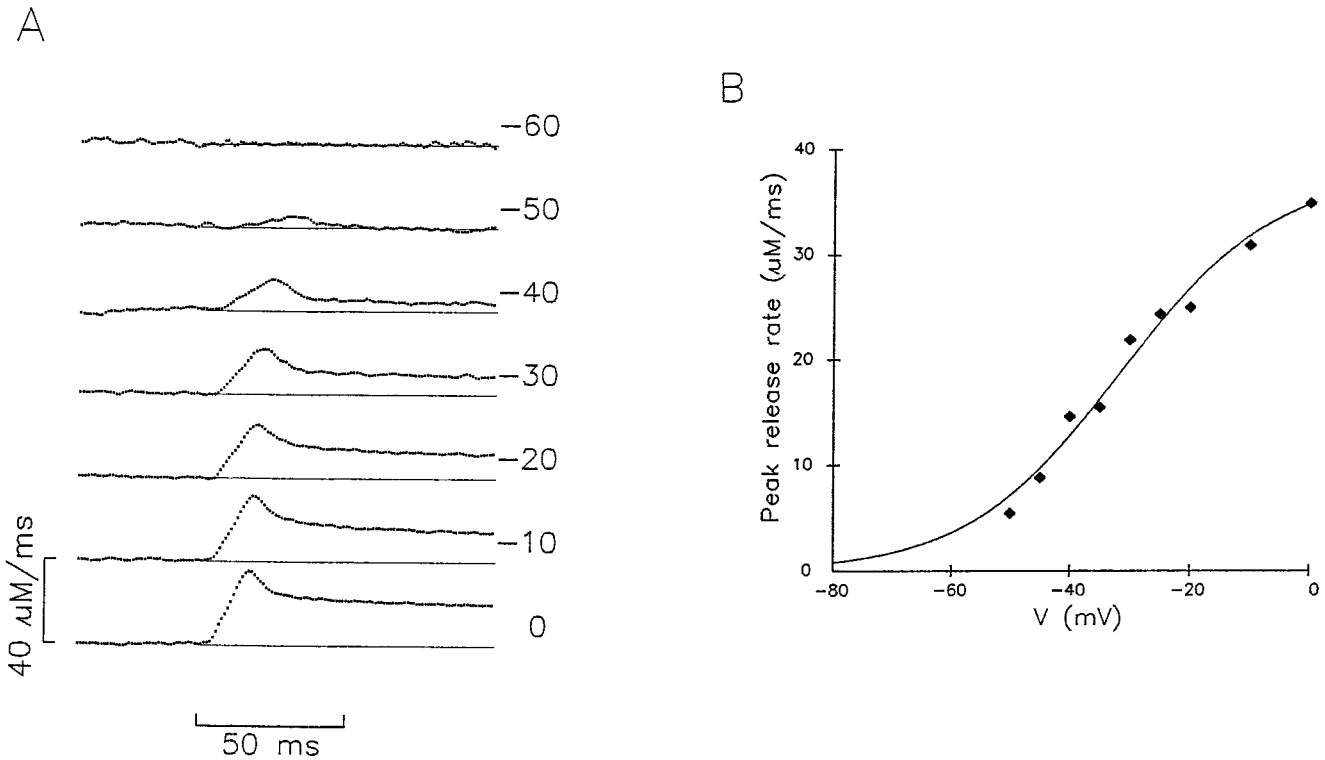

FIGURE 2 Calcium release in a cut fiber bathed in a TEA-Cl solution. Same experiment as in Fig. 1. (*A*) Calcium release rate traces obtained from time derivative of $\Delta[Ca_T]$ traces, some of which are shown in Fig. 1 *C*. The numbers to the right of the traces show the potentials during the test pulses. The thin straight lines mark the prestimulus baselines. (*B*) Plot of Rel_p versus the pulse potential. The smooth curve was obtained by least-squares fit of Eq. 1 to the points. The best-fit values for $\bar{V}$, k, and $Rel_{p,max}$ are −31.5 mV, 12.7 mV, and 37.7 μM ms^{-1}.

troponin, parvalbumin, and EGTA and the binding of Mg^{2+} to parvalbumin. The assumed values given in Methods for the binding constants and the concentrations of ligands were used in the computation.

Fig. 2 *A* shows traces of Rel (defined in Methods) obtained by taking time derivatives of the traces in Fig. 1 *C* and two others not shown. At ≤ -60 mV, there was no detectable calcium signal. The trace also appeared to be noisier than the later traces. That was due to the presence of a lower [ApIII] at the beginning of the pulse sequence. As the experiment progressed, more ApIII diffused into the myoplasm and the noise level improved. The first sign of calcium release appeared at around -50 mV. Above that potential, Rel followed a general waveform with an early peak and a maintained phase, similar to those published by other investigators (beginning with Kovacs et al., 1979, in cut fibers and Baylor et al., 1983a, in intact fibers). With increasing depolarizations, the amplitudes of both the early peak and the maintained phase became larger and the time to peak became shorter. The so-called maintained phase was actually decaying very slowly. This slow decay was more noticeable at larger depolarizations and was probably the result of the slow depletion of Ca^{2+} content in the SR, which was studied in some detail by various investigators (Jacquemond et al., 1991; Jong et al., 1993; Pape et al., 1995).

To study the voltage dependence of the peak amplitude of Rel, i.e., Rel_p, the values from the traces in Fig. 2 *A* and two others not shown are plotted as a function of potential in Fig. 2 *B*. The signal at -60 mV was too small to provide a meaningful value of Rel and so the point was omitted. The set of data points was fitted with a single Boltzmann distribution function,

$$Rel_p(V) = Rel_{p,max}\left\{1 + \exp\left(-\frac{V - \bar{V}}{k}\right)\right\}^{-1} \qquad (1)$$

in which $Rel_{p,max}$, V, and k represent the saturated value of Rel_p at large positive potentials, the equidistribution potential, and the voltage dependence (or inverse steepness) factor, respectively. The best-fit curve so obtained is represented by the smooth curve in Fig. 2 *B*. The best-fit values of the respective parameters are given in the figure legend. Similar measurement of calcium release in the TEA-Cl external solution was carried out in nine other fibers and the results were close to that shown in Fig. 2. The average values of the Boltzmann parameters are listed in the first row of Table 2. The next four figures in the following sections follow the same layout as in Fig. 2 and the corresponding values of the Boltzmann parameters are listed in Table 2 for comparison.

Comparison of calcium release in external solutions containing different anions

To minimize anionic current in skeletal muscle fibers under voltage clamp, $CH_3SO_3^-$ has been routinely used to replace the Cl^- in the external solution by many investigators. Fig. 3 shows an experiment performed to study calcium release in a fiber bathed in this solution. The Rel traces shown in Fig. 3 *A* resemble those in TEA-Cl solution (Fig. 2 *A*) except for a shift in the threshold. Specifically, although no calcium release signal was detected at -60 mV in Fig. 2 *A*, the signal was noticeable at the same potential in Fig. 3 *A*.

The values of Rel_p from the traces in Fig. 3 *A*, and others not shown, are plotted against potential in Fig. 3 *B*. The smooth curve was obtained by least-squares fit of Eq. 1 to the points. From the best-fit values listed in the figure legend, one gets the impression that the value of V in $CH_3SO_3^-$ is more negative than that in Cl^-, which agrees with the shift in the threshold of calcium release mentioned above. However, this difference existed only between the pair of fibers in Figs. 2 and 3 (see next paragraph). Also, the value of $Rel_{p,max}$ in $CH_3SO_3^-$ is smaller than that in Cl^-.

The experiment of Fig. 3 was repeated in 21 other fibers and the results were similar. The average values of the Boltzmann parameters are listed in the second row of Table 2. The average value of $Rel_{p,max}$ in Cl^- is 39% larger than that in $CH_3SO_3^-$. The difference is statistically significant ($P < 0.01$, Student's two-tailed *t*-test). On the other hand, the differences between the average values of V and k in the

TABLE 2 Comparison of voltage dependence of peak release rate in different external solutions

External solution	N	$\bar{V}$ (mV)	k (mV)	$Rel_{p,max}$ (μM ms^{-1})
I. Nominal $[Ca^{2+}]_i$ = 50 nM				
Cl^- (E)	10	-38.5 ± 2.0	10.4 ± 0.6	37.5 ± 2.0
$CH_3SO_3^-$ (F)	22	-37.2 ± 1.4	11.0 ± 0.3	27.0 ± 1.9
Gluconate (I)	3	-41.7 ± 4.5	9.6 ± 0.7	29.8 ± 2.5
Calcium-free $CH_3SO_3^-$ (G)	21	-34.1 ± 1.0	9.7 ± 0.4	18.9 ± 1.9
Calcium-free gluconate	10	-43.1 ± 1.7	10.2 ± 0.7	15.1 ± 1.3
Calcium-free SO_4^{2-} (H)	3	-38.8 ± 1.9	8.0 ± 0.3	16.5 ± 4.7
II. Nominal $[Ca^{2+}]_i$ = 10 nM				
Cl^- (E)	3	-44.1 ± 4.3	7.7 ± 1.5	29.7 ± 0.8
$CH_3SO_3^-$ (F)	3	-44.9 ± 5.6	6.8 ± 1.7	17.6 ± 4.7

Column 1 lists the major anions in the calcium-containing and calcium-free external solutions. Letters in parentheses after the anions indicate the corresponding solutions listed in Table 1. Column 2 gives the number of fibers studied in each solution. The Rel_p-V plot from each fiber was least-squares fitted by Eq. 1. Columns 3–5 give the mean and SEM of the best-fit values of the parameters from the fibers in each solution.

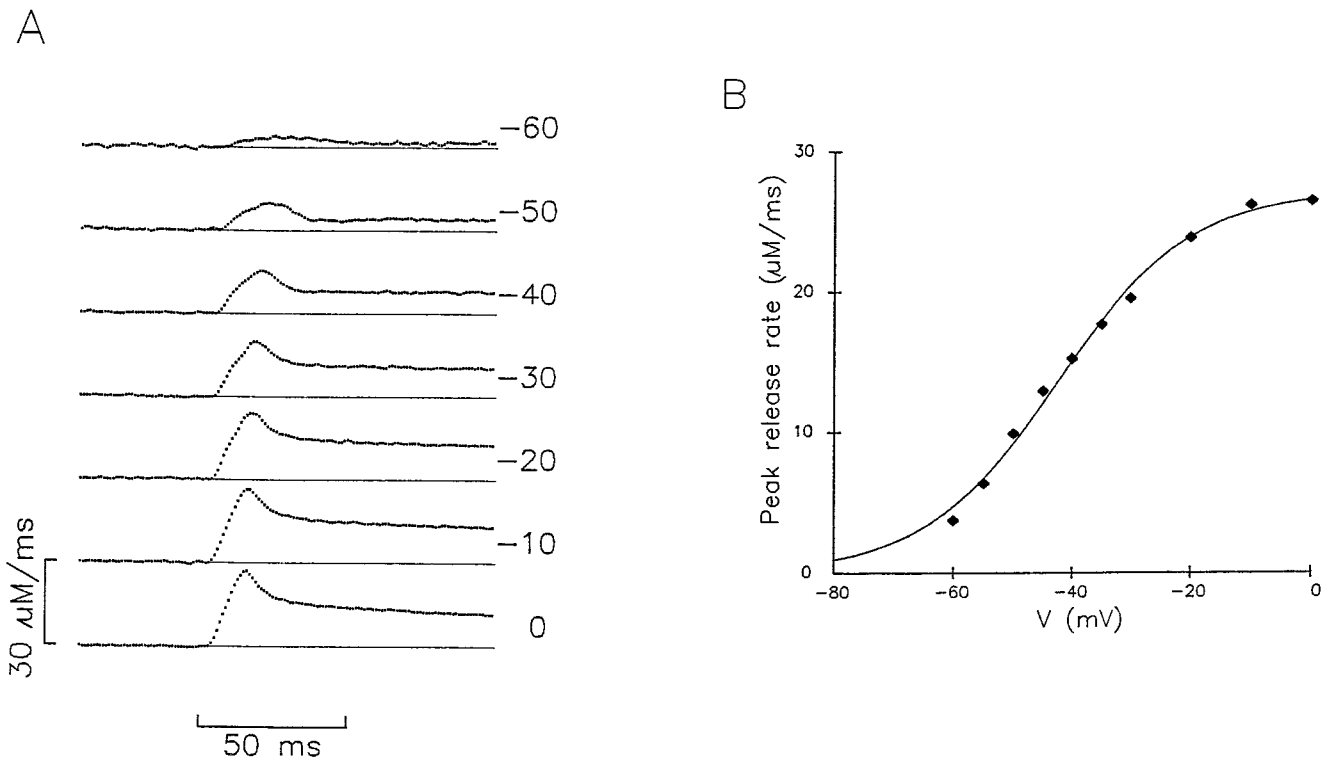

FIGURE 3 Calcium release in a cut fiber bathed in a TEA-CH_3SO_3 solution. The end pools contained solution B and the center pool contained solution F. From the beginning to the end of the experiment, the holding current changed from −48 to −51 nA and $r_e/(r_e + r_i)$ decreased from 0.974 to 0.972. At the 49th minute, 0.65 mM ApIII was added to the end pools. At the 93rd minute, the [ApIII] in the end pools was reduced to 0.29 mM. (*A*) Representative calcium release rate traces taken from the 103rd to the 128th minute, during which the myoplasmic [ApIII] increased from 0.63 to 0.81 mM. The numbers to the right of the traces show the potentials during the test pulses. The thin straight lines mark the prestimulus baselines. (*B*) Plot of Rel_p versus the pulse potential. The smooth curve was obtained by least-squares fit of Eq. 1 to the points. The best-fit values for $\bar{V}$, *k*, and $Rel_{p,max}$ are −42.5 mV, 11.2 mV, and 27.1 μM ms^{-1}. Fiber diameter = 91 μm; sarcomere length = 4 μm.

two solutions are not statistically significant ($P > 0.5$ and 0.2, respectively, Student's two-tailed *t*-test). Thus, the shift in V between the two solutions observed above did not hold when the parameter was averaged over two groups of fibers.

Calcium release was also studied in a TEA-gluconate external solution. Because gluconate chelates Ca^{2+}, the amount of total calcium in the solution was increased to 10 mM to adjust the free [Ca^{2+}] to 1.8 mM, which was checked with a calcium-sensitive electrode. Calcium release in this calcium-containing TEA-gluconate external solution was studied in three fibers. Results from one of the experiments are shown in Fig. 4.

From the Rel traces shown in Fig. 4 *A*, it can be observed that the amplitudes of Rel_p were quite comparable to those in Fig. 3 *A*. What distinguishes the waveforms of Rel in the two solutions is the decay phases of the traces. In the traces of Fig. 3 *A*, Rel decayed to a more or less maintained level after the early peak. The decay was almost absent in the traces of Fig. 4 *A*, resulting in a higher maintained level. In the other two fibers studied in the TEA-gluconate solution, the decay of Rel to the maintained level was slightly more pronounced than that in the traces of Fig. 4 *A* but less than that in the traces of Fig. 3 *A*, suggesting that the decay is less in gluconate than in $CH_3SO_3^-$. It will be seen later in Fig. 8 that the decay is even larger in Cl^- than in $CH_3SO_3^-$, but because of fiber-to-fiber variation, this difference cannot be detected in comparing the traces of Figs. 2 *A* and 3 *A*.

The values of Rel_p from the traces in Fig. 4 *A* and others not shown are plotted against potential in Fig. 4 *B* and least-squares fitted with Eq. 1. The best-fit values of the Boltzmann parameters are listed in the figure legend. The average best-fit values of the parameters from the three fibers are listed in the third row of Table 2. The differences between these average values and those in $CH_3SO_3^-$ are not statistically significant ($P > 0.5$, 0.2, and 0.1 for $Rel_{p,max}$, $\bar{V}$, and k, respectively, Student's two-tailed *t*-test). The general conclusion in this section is that the value of $Rel_{p,max}$ in Cl^- is larger than those in impermeant anions, irrespective of which impermeant anion was used.

Effects of $[Ca^{2+}]_o$ on calcium release

In experiments employing long depolarizing pulses, a calcium-free external solution has often been used to avoid inward Ca^{2+} current. It is thus of interest to find out whether the replacement of Ca^{2+} with Mg^{2+} in the external solution affects calcium release in those fibers. The first group of

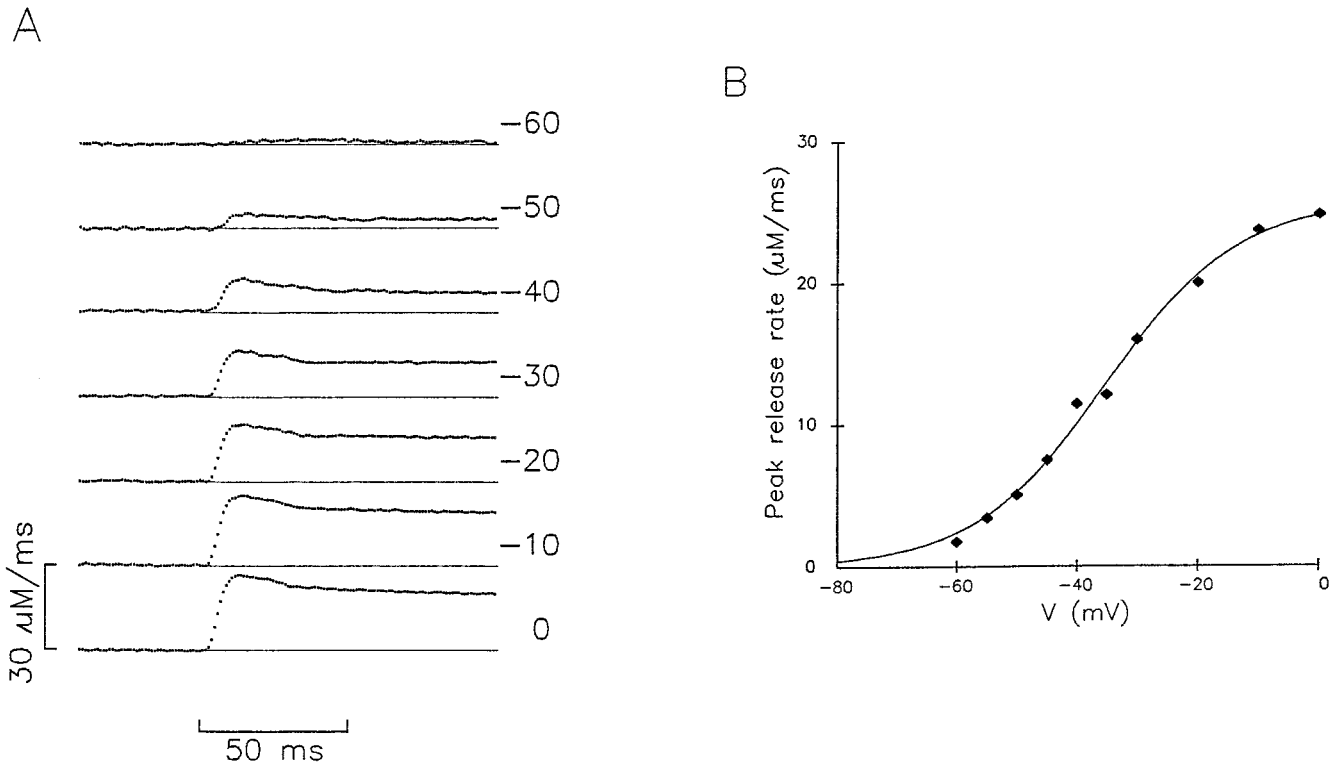

FIGURE 4 Calcium release in a cut fiber bathed in a TEA-gluconate solution. The end pools contained solution B and the center pool contained solution I. From the beginning to the end of the experiment, the holding current changed from −38 to −39 nA and $r_e/(r_e + r_i)$ decreased from 0.982 to 0.981. At the 49th minute, 1.67 mM ApIII was added to the end pools. (*A*) Representative calcium release rate traces taken from the 101st to the 119th minute, during which the myoplasmic [ApIII] increased from 0.69 to 0.85 mM. The numbers to the right of the traces show the potentials during the test pulses. The thin straight lines mark the prestimulus baselines. (*B*) Plot of Rel_p versus the pulse potential. The smooth curve was obtained by least-squares fit of Eq. 1 to the points. The best-fit values for $\bar{V}$, k, and $Rel_{p,max}$ are −35.1 mV, 10.9 mV, and 25.7 μM ms^{-1}. Fiber diameter = 98 μm; sarcomere length = 4 μm.

experiments in this category was performed in a calcium-free TEA-CH_3SO_3 external solution. Calcium release was elicited by a sequence of test pulses. The computed Rel signals are shown in Fig. 5 *A*. The traces resemble those in Fig. 3 *A*, but differ in two minor respects, namely the magnitudes of the peaks were smaller and the time course of the peaks were slower in the traces of Fig. 5 *A*. The values of Rel_p from these traces, and others not shown, are plotted against potential in Fig. 5 *B* and least-squares fitted with Eq. 1. The best-fit values of the Boltzmann parameters are listed in the figure legend. The value of 20.5 μM ms^{-1} for $Rel_{p,max}$ in this experiment is smaller than the 27.1 μM ms^{-1} obtained in the calcium-containing TEA-CH_3SO_3 solution (Fig. 3).

Twenty-one experiments were performed in the calcium-free TEA-CH_3SO_3 solution. The average best-fit values of the Boltzmann parameters are listed in the fourth row of Table 2. The difference in $Rel_{p,max}$ in the calcium-containing and calcium-free TEA-CH_3SO_3 solutions still holds between the two average values and the difference is statistically significant ($P < 0.01$, Student's two-tailed t-test).

The effect of external [Ca^{2+}] on calcium release was also studied in gluconate. Calcium release was measured in ten fibers bathed in a calcium-free TEA-gluconate solution. This solution is not listed in Table 1, but was prepared by replacing the 10 mM total calcium in the calcium-containing gluconate solution (solution I) with the same amount of magnesium. The calcium release signal appeared to be quite normal (traces not shown). The average best-fit values of the Boltzmann parameters from the Rel_p-V curves are listed in the fifth row of Table 2. The average value of $Rel_{p,max}$ in the calcium-containing solution is again larger than that in the calcium-free solution and the difference is also statistically significant ($P < 0.001$, Student's two-tailed t-test). Combining the results from the experiments in $CH_3SO_3^-$ and gluconate, it can be concluded that extracellular Ca^{2+} plays a role in influencing the early phase of Rel. This is not due to the absence of divalent cation because Mg^{2+} was used to replace the Ca^{2+}.

Another group of three experiments was performed in a calcium-free $(TEA)_2SO_4$ solution. The computed Rel traces from one of experiments are shown in Fig. 6 *A*. The peak amplitudes of these traces were smaller than those in calcium-free TEA-CH_3SO_3 solution. Also, the waveform of the signals in Fig. 6 *A* was somewhat unusual. Rel rose rapidly on depolarization and was slowed down halfway before reaching the peak, resulting in a convex slope in the rising phase. This feature was not shared by the other two fibers in the same solution and thus is not a characteristic of calcium release in the calcium-free $(TEA)_2SO_4$ solution. In

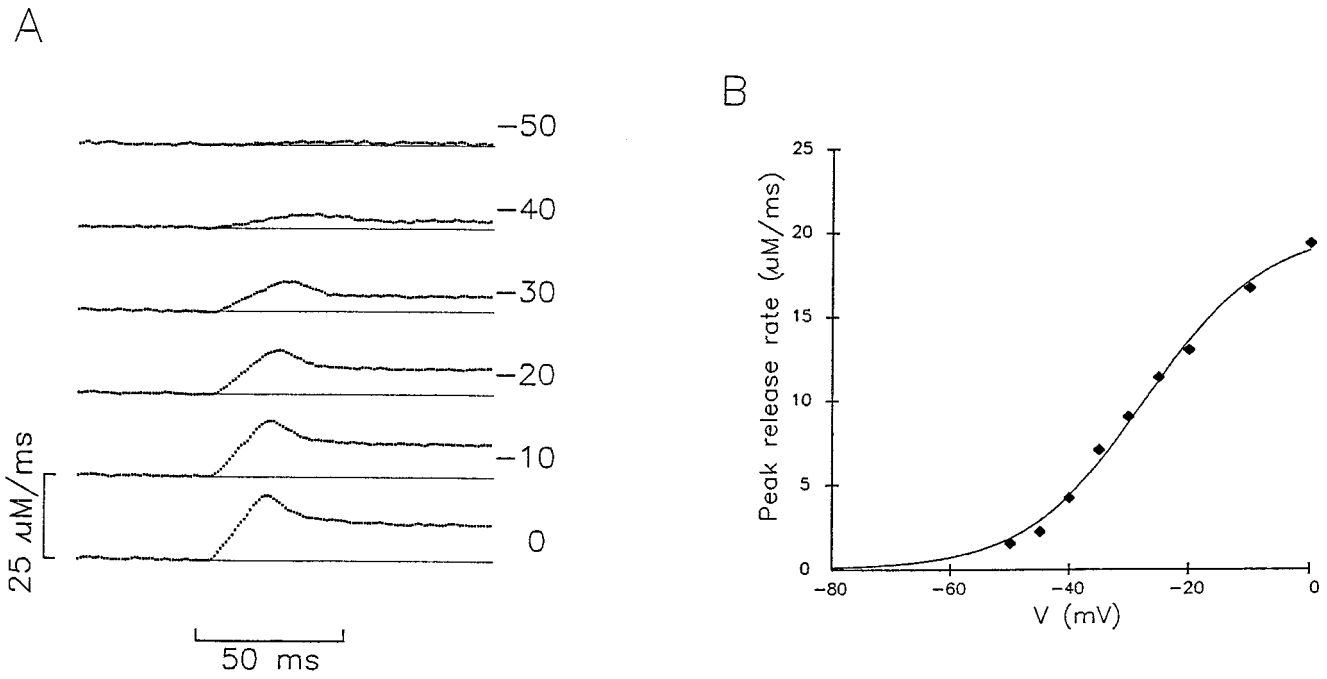

FIGURE 5 Calcium release in a cut fiber bathed in a calcium-free TEA-CH_3SO_3 solution. The end pools contained solution B and the center pool contained solution G. From the beginning to the end of the experiment, the holding current remained constant at −44 nA and $r_e/(r_e + r_i)$ increased from 0.968 to 0.969. At the 60th minute, ApIII was added to the end pools, but the [ApIII] was not measured. (*A*) Representative calcium release rate traces taken from the 142nd to the 178th minute, during which the myoplasmic [ApIII] increased from 0.64 to 0.96 mM. The numbers to the right of the traces show the potentials during the test pulses. The thin straight lines mark the prestimulus baselines. (*B*) Plot of Rel_p versus the pulse potential. The smooth curve was obtained by least-squares fit of Eq. 1 to the points. The best-fit values for $\bar{V}$, k, and $Rel_{p,max}$ are −26.9 mV, 10.2 mV, and 20.5 μM ms^{-1}. Fiber diameter = 80 μm; sarcomere length = 4 μm.

fact, a similar convex-shaped rising phase was observed in the calcium-free TEA-CH_3SO_3 solution. Thus, the presence or absence of convexity is due to fiber-to-fiber variation.

The values of Rel_p from the traces in Fig. 6 *A*, and others not shown, are plotted against potential in Fig. 6 *B*. The smooth curve was obtained by least-squares fit of Eq. 1 to the points. The best-fit values of the Boltzmann parameters are listed in the figure legend. The best-fit values of the Boltzmann parameters in the calcium-free $(TEA)_2SO_4$ solution, averaged over the three fibers, are listed in the sixth row of Table 2. The differences between this average value of $Rel_{p,max}$ and those in the calcium-free TEA-CH_3SO_3 and calcium-free gluconate solutions are not statistically significant ($P > 0.5$ in both comparisons, Student's two-tailed *t*-test). This finding substantiates the conclusion given above that the choice of the impermeant anion does not affect the early rate of calcium release in calcium-containing external solutions.

Effects of $[Ca^{2+}]_i$ on calcium release

The presence of intracellular Ca^{2+} should play an important role in calcium release, because it affects directly the loading of Ca^{2+} into the SR. All the experiments described in the preceding sections were performed on fibers containing 20 mM EGTA and 1.8 mM total calcium. The free myoplasmic $[Ca^{2+}]$ in that solution was estimated to be 50 nM, which will be referred to as normal $[Ca^{2+}]_i$. Many other experiments were performed on fibers containing 20 mM EGTA without any added calcium, in which case the free myoplasmic $[Ca^{2+}]$ was nominally $<10^{-12}$ M. In those experiments, hardly any ApIII absorbance signal could be detected when the fibers were stimulated. This can be explained by the fact that, in the early stage of the experiment, [ApIII] was low and most of the released Ca^{2+} was chelated by EGTA and forbidden from reaching the few ApIII molecules. Later on, because there was hardly any free Ca^{2+} in the myoplasm, the SR Ca^{2+} content was depleted after some depolarizations. Thus, although [ApIII] was increased, the amount of released Ca^{2+} was greatly reduced.

Between the two extremes of zero and normal $[Ca^{2+}]_i$, substantial calcium release can be detected at an intermediate $[Ca^{2+}]_i$, as shown in Fig. 7 *A*. The experiment was carried out in the calcium-containing TEA-CH_3SO_3 external solution. Initially, the internal solution contained 20 mM EGTA plus 0.4 mM total calcium. The free myoplasmic $[Ca^{2+}]$ was estimated to be 10 nM, which will be referred to as reduced $[Ca^{2+}]_i$. Although the traces were noisy, because the myoplasmic [ApIII] was below 0.62 mM, they showed that Rel was quite sizable. Subsequently, the total calcium in the internal solution was increased to the usual 1.8 mM. More than 30 min was allowed for the Ca^{2+} to diffuse into the myoplasm. The traces in Fig. 7 *B* were then taken. They

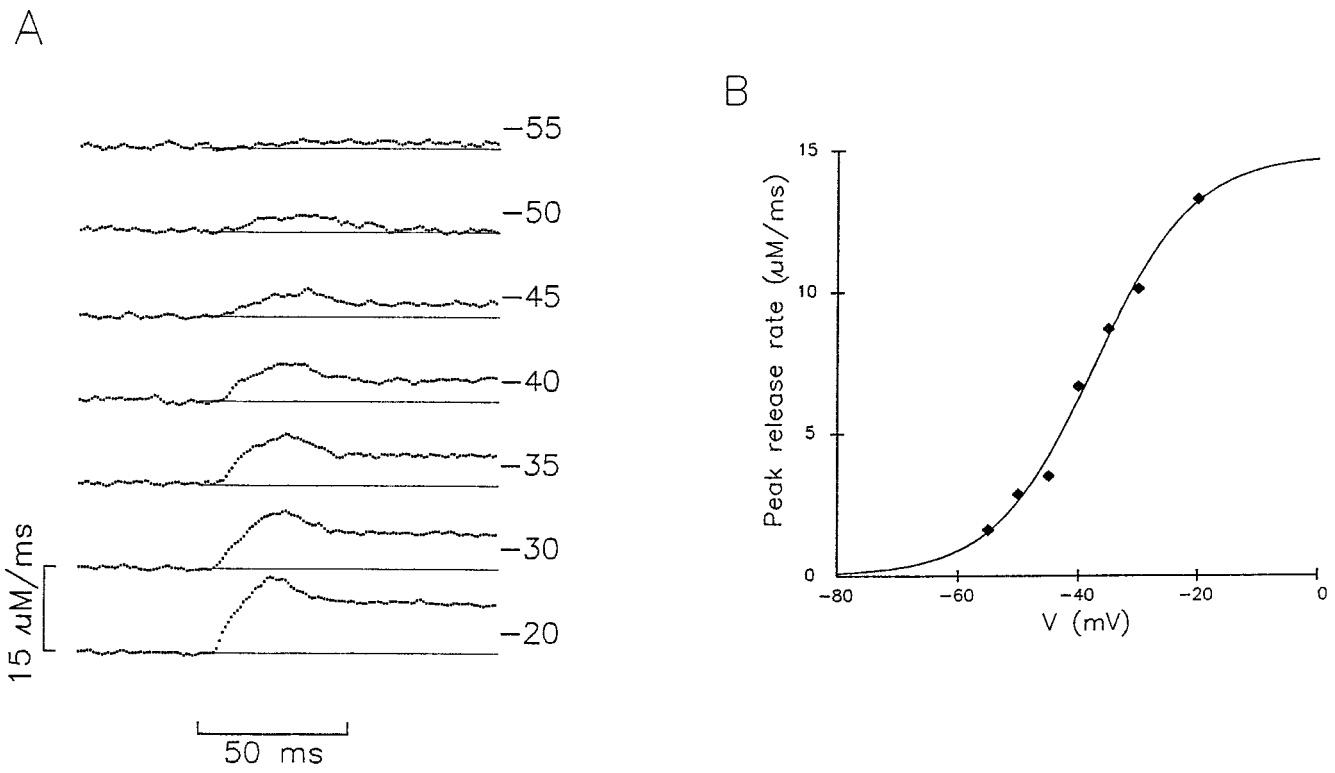

FIGURE 6 Calcium release in a cut fiber bathed in a calcium-free $(TEA)_2SO_4$ solution. The end pools contained solution D and the center pool contained solution H. From the beginning to the end of the experiment, the holding current changed from −50 to −53 nA and $r_e/(r_e + r_i)$ decreased from 0.981 to 0.980. At the 57th minute, 0.69 mM ApIII was added to the end pools. At the 136th minute, the [ApIII] in the end pools was reduced to 0.20 mM. (*A*) Representative calcium release rate traces taken from the 173rd to the 199th minute, during which the myoplasmic [ApIII] increased from 0.62 to 0.68 mM. The numbers to the right of the traces show the potentials during the test pulses. The thin straight lines mark the prestimulus baselines. (*B*) Plot of Rel_p versus the pulse potential. The smooth curve was obtained by least-squares fit of Eq. 1 to the points. The best-fit values for $\bar{V}$, k, and $Rel_{p,max}$ are −37.3 mV, 8.3 mV, and 14.8 μM ms^{-1}. Fiber diameter = 105 μm; sarcomere length = 4.2 μm.

appeared much smoother because the [ApIII] had increased substantially, up to 1.52 mM at the end of the experiment.

To compare the waveforms of the Rel signals in the presence of the two different $[Ca^{2+}]_i$, the pair of traces at −30 mV (or −10 mV) in Fig. 7, *A* and *B*, are normalized and superimposed in the upper (or lower) panel of Fig. 7 *C*. In each panel, the trace that peaks earlier and decays faster is the one taken with reduced $[Ca^{2+}]_i$. The times to peak were 15.1 and 19.7 ms in the two traces of the upper panel and 12.5 and 16.4 ms in the two traces of the lower panel. Following the peak in each trace, the decay appeared to have a fast and a slow component. The origin of the fast decay will be discussed in the next section. The slow decay probably reflects the depletion of the Ca^{2+} content in the SR. To separate the two components, the decay phase of each trace was fitted with a sum of two exponentials with time constants τ_1 and τ_2. The fitting routine was set up in a way such that the iteration was terminated as soon as the longer time constant τ_2 exceeded 2000. Because of the uncertainties involved in estimating free $[Ca^{2+}]$ with ApIII at late times (see Discussion), the values of τ_2 can only be used for qualitative comparison.

In the upper panel, τ_1 was increased from 5.1 ms with reduced $[Ca^{2+}]_i$ to 8.1 ms with normal $[Ca^{2+}]_i$ and τ_2 was increased from 77 ms with reduced $[Ca^{2+}]_i$ to > 2000 ms with normal $[Ca^{2+}]_i$. In the lower panel, τ_1 was increased from 7.5 ms with reduced $[Ca^{2+}]_i$ to 7.8 ms with normal $[Ca^{2+}]_i$ and τ_2 was increased from 54 ms with reduced $[Ca^{2+}]_i$ to 284 ms with normal $[Ca^{2+}]_i$. Although only two pairs of traces are shown, similar changes occurred in other pairs. The small increase in τ_1 from one trace to the other was probably caused by fiber run-down, as reflected by the slower rise time and the longer time to peak. The large increase in τ_2 is more interesting. In the presence of reduced $[Ca^{2+}]_i$, the SR Ca^{2+} content was likely reduced. The calcium store should be depleted faster during depolarization, and thus the maintained phase of Rel should decay faster. After the $[Ca^{2+}]_i$ was brought back to normal, the calcium store was replenished to some extent, and thus the maintained phase of Rel should decay more slowly. This probably explains the observed increases in τ_2.

To gain some information about the voltage dependence of early calcium release in fibers with reduced $[Ca^{2+}]_i$, the values of Rel_p from the traces in Fig. 7 *A* were plotted against potential (not shown) and fitted with Eq. 1. Similar plots were obtained from two other fibers bathed in the calcium-containing $TEA\text{-}CH_3SO_3$ solution. The best-fit values of the Boltzmann parameters, averaged over the three

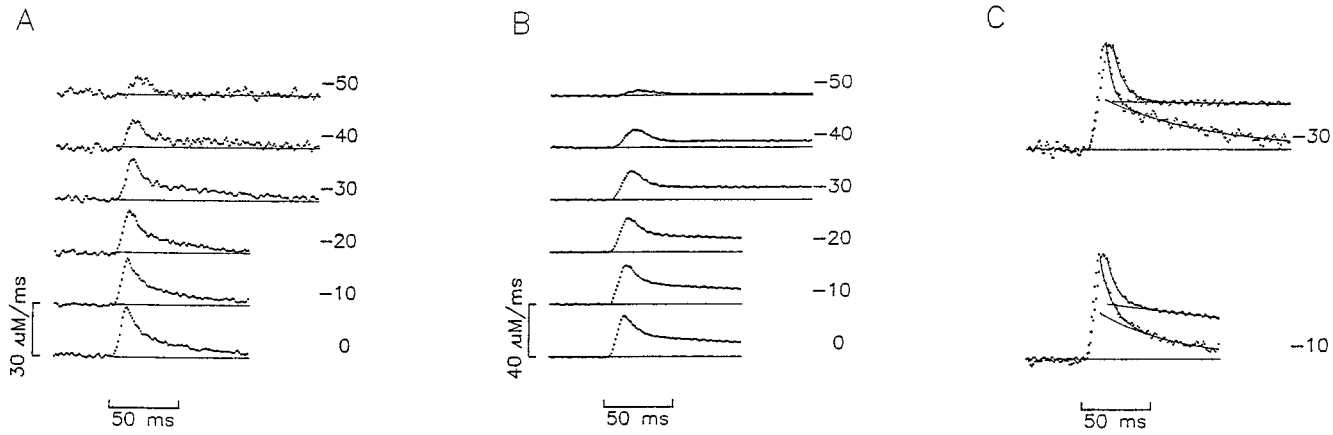

FIGURE 7 Comparison of calcium release signals in a cut fiber containing reduced and normal levels of $[Ca^{2+}]_i$. The center pool contained solution F. Initially, the end pools contained solution C. From the beginning to the end of the experiment, the holding current changed from −33 to −41 nA and $r_e/(r_e + r_i)$ decreased from 0.973 to 0.964. At the 52nd minute, 0.67 mM ApIII was added to the end pools. (*A*) Representative traces taken from the 79th to the 95th minute, during which the myoplasmic [ApIII] increased from 0.12 to 0.62 mM. At the 109th minute, the end-pool solution was changed to solution D. (*B*) Representative traces taken from the 144th to the 160th minute, during which the myoplasmic [ApIII] increased further to 1.52 mM. (*C*) Each pair of traces at −30 and −10 mV from (*A*) and (*B*) are superimposed, with normalized peak amplitude, on expanded scales. The traces in reduced $[Ca^{2+}]_i$ are those with earlier peaks in each pair. A sum of two exponentials was fitted to the decay phase of each trace, as indicated by the two smooth curves superimposed on the trace. The numbers to the right of the traces show the potentials during the test pulses. The thin straight lines mark the prestimulus baselines. Fiber diameter = 71 μm; sarcomere length = 3.8 μm.

fibers, are listed in the eighth row of Table 2. In comparing the averaged value of $Rel_{p,max}$ in this row with that in the second row, it appears that the reduction in $[Ca^{2+}]_i$ diminished the peak rate of calcium release. While this may be true, the difference is not statistically significant ($P > 0.05$, Student's two-tailed *t*-test).

Similar comparison of calcium release was carried out in the TEA-Cl external solution. Calcium release was studied in three fibers with reduced $[Ca^{2+}]_i$. The average best-fit values of the Boltzmann parameters are listed in the seventh row of Table 2. Again, in comparing the averaged value of $Rel_{p,max}$ in this row with that in the first row, the reduction in $[Ca^{2+}]_i$ diminished the peak rate of calcium release, but again the difference is not statistically significant ($P > 0.05$, Student's two-tailed *t*-test). Combining the results from the TEA-CH_3SO_3 and TEA-Cl experiments, it can be concluded that a reduction in the myoplasmic free $[Ca^{2+}]$ affects the rate of Ca^{2+} depletion in the SR more than Rel_p. This is puzzling, because if the SR is less depleted with releasable Ca^{2+} in fibers with 50 nM $[Ca^{2+}]_i$, it is difficult to imagine why Rel_p is not increased more than what was observed. This apparent discrepancy could be partially explained by the fact that, although the SR was more loaded, the myoplasmic $[Ca^{2+}]$ was also increased. Thus, the gradient of free $[Ca^{2+}]$ across the SR membrane might not have changed appreciably. In addition, if more Ca^{2+} is released when the SR is more loaded, it can cause a larger inactivation of the release and thus suppress the peak.

Effect of replacing external Cl^- with $CH_3SO_3^-$ on calcium release waveform

Another interesting observation was made on a fiber exposed to the calcium-containing TEA-Cl and TEA-CH_3SO_3 external solutions. The traces shown in Fig. 8 *A* were elicited by constant pulses to −30 mV. A comparison of Rel_p in the two solutions at a fixed potential is justified because there is no apparent shift in the voltage dependence of Rel_p between the two solutions (column 3 of first and second rows in Table 2). Initially, the fiber was bathed in the TEA-Cl solution. After the first trace was taken, the external solution was changed to the one containing TEA-CH_3SO_3 and the next three traces were taken. (Many traces were taken in between at other potentials but are not shown.) The peak amplitude in trace 2 was reduced by 20% from that of trace 1 and was reduced further in traces 3 and 4, probably due in part to run-down. Finally, the external solution was changed back to the control and the last trace was taken. The peak amplitude in trace 5 was increased by 24% from that of trace 4, suggesting that the attenuating effect of $CH_3SO_3^-$ was at least partially reversible.

To compare the waveforms of the traces, the top (or bottom) two traces are normalized and superimposed in the upper (or lower) panel in Fig. 8 *B*. In each panel, the trace that peaks earlier and decays faster is the one taken in Cl^-. The decay phase of each trace was fitted with a sum of two exponentials with time constants τ_1 and τ_2, as was done in Fig. 7 *B*. The values of τ_2 in all the traces were >2000 ms. The upper panel shows that $CH_3SO_3^-$ increased the time to peak and the increase was reversed in the lower panel when Cl^- was restored, suggesting that the increase was probably not due to run-down. In contrast to its suppressing effect on the peak amplitude, $CH_3SO_3^-$ increased the amplitude of the maintained phase (upper panel) and the increase was also reversible (lower panel). Many other experiments were performed, but in all of them, only one solution change was made, either from Cl^- to $CH_3SO_3^-$ or from $CH_3SO_3^-$ to Cl^-.

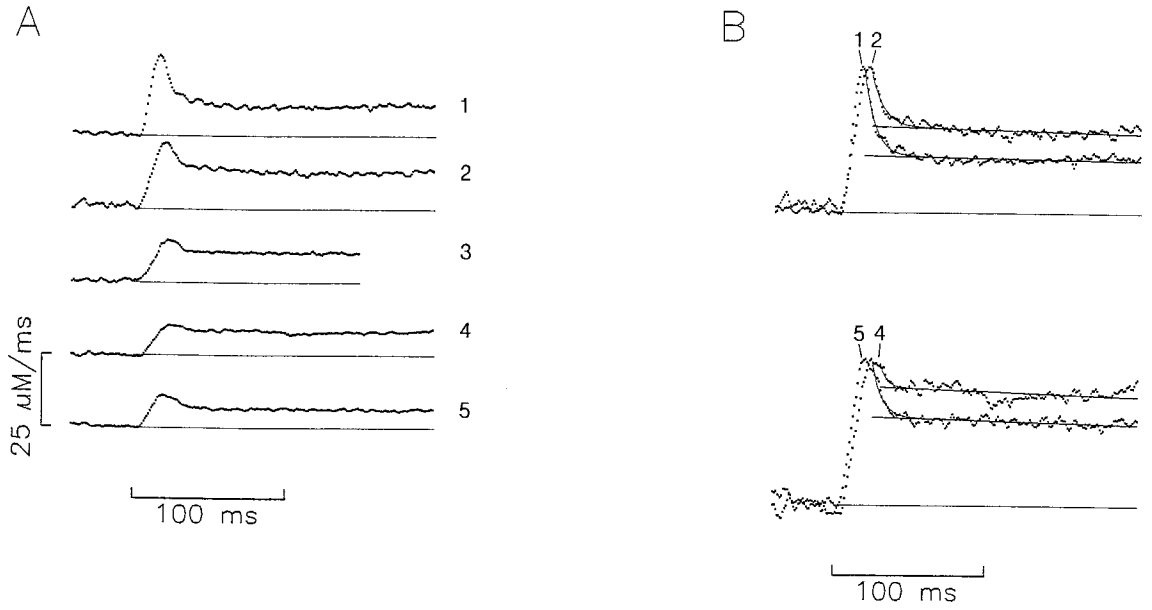

FIGURE 8 Comparison of calcium release signals in TEA-Cl and TEA-CH_3SO_3 external solutions. The end pools contained solution B. Initially, the center pool contained solution E. From the beginning to the end of the experiment, the holding current changed from −27 to −33 nA and $r_e/(r_e + r_i)$ remained unchanged at 0.974. At the 64th minute, 0.42 mM ApIII was added to the end pools. (*A*) Representative traces elicited by a constant test pulse to −30 mV. Trace 1 was taken at the 157th minute. At the 159th minute, the solution in the center pool was changed to solution F. Traces 2 through 4 were taken from the 172nd to the 210th minute. The pulse that elicited trace 3 lasted only 150 ms. At the 212nd minute, the solution in the center pool was changed back to solution E. Trace 5 was taken at the 222nd minute. From the first to the fifth trace, the myoplasmic [ApIII] increased from 0.52 to 0.78 mM. The peak amplitudes from traces 1 through 5 are 26.5, 21.2, 15.3, 10.2, and 12.6 μM ms^{-1}, respectively. (*B*) Superpositions of two pairs of Ca traces, with normalized peak amplitude, on expanded scales. The upper pair are from traces 1 and 2 and the lower pair from traces 4 and 5 in (*A*). The trace with earlier peaks in each pair is the one in Cl^-. A sum of two exponentials was fitted to the decay phase of each trace, as indicated by the two smooth curves superimposed on the trace. The values of τ_2 are >2000 ms in all the traces. The values of time to peak, amplitude of plateau, and τ_1, are: for trace 1, 16.2 ms, 9.8 μM ms^{-1}, and 7.0 ms; for trace 2, 20.4 ms, 13.5 μM ms^{-1}, and 7.9 ms; for trace 4, 25.9 ms, 8.5 μM ms^{-1}, and 4.5 ms; for trace 5, 19.6 ms, 5.7 μM ms^{-1}, and 6.5 ms. The thin straight lines mark the prestimulus baselines. Fiber diameter = 69 μm; sarcomere length = 4 μm.

The results from those experiments were similar to those shown in Fig. 8.

DISCUSSION

Choice of calcium indicator

In this article, calcium release was studied with ApIII as the indicator. ApIII might not be the best choice, as it is known to be sensitive to a change in pH. Because of this, data analysis was focused on the early peak of the release waveform, when the contamination due to pH change is minimal. It is also believed that ApIII would lead to an underestimation, by severalfold, of the change in myoplasmic free $[Ca^{2+}]$, when compared with the value obtained with a lower-affinity indicator, PDAA (Hirota et al., 1989), thereby creating some uncertainties in the calculation of Rel waveform. Nonetheless, ApIII is one of the most commonly used and readily available absorbance indicators. It is still useful for qualitative comparison, as long as the measurement is confined to a short time after depolarization.

Voltage dependence of peak release rate

The voltage dependence of Rel_p was studied in cut fibers exposed to various internal and external solutions. In the experiments reported in this article, calcium release was elicited up to 0 mV or less to avoid excessive damage on the fibers. Within this potential range, the Rel_p-V plot can be fitted reasonably well with a single Boltzmann distribution function. It should be noted that calcium release at just suprathreshold potentials was not included in the analysis because the signal could not be measured reliably. Had the measurements been available, they should contribute a steep component to the foot of the Rel_p-V curve.

Comparison with published results

Very little information on the Rel_p-V relationship is available from published works on calcium release in frog muscle fibers. Some studies were limited to the voltage dependence of Rel_p at just suprathreshold potentials. To my knowledge, Melzer et al. (1986) were the first group of investigators who studied calcium release in a potential range wide enough to allow them to fit a Boltzmann distribution function to the Rel_p-V plot. They obtained best-fit values of +3.1 mV, 13.6 mV, and 2.7 μM ms^{-1} for $\bar{V}$, k, and $Rel_{p,max}$, respectively, from one fiber bathed in a calcium-containing SO_4^{2-} external solution. Their value of $Rel_{p,max}$ was very small. Subsequently, Klein et al. obtained averaged values of −44.3 mV, 10.3 mV, and 27.3 μM ms^{-1}

(1990) and −40.0 mV, 9.3 mV, and 19.9 μM ms^{-1} (1992) for the respective Boltzmann parameters from fibers bathed in the same external solution. These two sets of values are quite close to the set shown in the second row of Table 2 from fibers bathed in the calcium-containing $CH_3SO_3^-$ external solution.

Ionic environments in the external and internal solutions affect $Rel_{p,max}$

Effect of major external anion

In fibers containing normal $[Ca^{2+}]_i$ and $[Ca^{2+}]_o$, the values of $Rel_{p,max}$ obtained when the external solutions contain different impermeant anions as the major anion are similar (second and third rows of Table 2). In contrast, when a calcium-containing external solution contains Cl^- as the major anion, the value of $Rel_{p,max}$ is significantly larger (first row). The lack of difference in the values of $Rel_{p,max}$ also holds for calcium-free external solutions containing different impermeant anions (fourth to sixth rows), although experiments employing a calcium-free Cl^- external solution have not yet been performed. This suggests that the rate of calcium release from the SR is larger if and only if the fiber is bathed in a Cl^- external solution. This finding is interesting and also reasonable, as it shows that muscle fibers are, by their nature, capable of utilizing the abundant external anion to enhance calcium release.

Effect of external Ca^{2+}

Table 2 shows that the value of $Rel_{p,max}$ is larger in a calcium-containing $CH_3SO_3^-$ external solution (second row) than that in a calcium-free $CH_3SO_3^-$ external solution (fourth row) and that the difference is statistically significant. Similarly, the value of $Rel_{p,max}$ is larger in a calcium-containing gluconate external solution (third row) than that in a calcium-free gluconate external solution (fifth row) and the difference is also statistically significant. This implies that the SR Ca^{2+} content in a calcium-free external solution is probably less full than that in a calcium-containing external solution. This agrees with the general understanding that although external Ca^{2+} is not required for the immediate triggering of calcium release (Armstrong et al., 1972), Ca^{2+} entry from the extracellular space replenishes the SR Ca^{2+} store in the long run after intense activities.

Effect of internal Ca^{2+}

Because intracellular Ca^{2+} affects the SR Ca^{2+} loading directly, it is anticipated to influence the rate of calcium release. In fact, when the internal solution is made calcium-free by the addition of 20 mM EGTA, very little calcium signal can be detected, but one does not have to go to this extreme to observe the effect. A comparison of the first and seventh (or second and eighth) rows in Table 2 shows that when the nominal $[Ca^{2+}]_i$ is reduced from 50 to 10 nM, the value of $Rel_{p,max}$ from fibers bathed in a calcium-containing Cl^- (or $CH_3SO_3^-$) external solution is reduced, although the difference is not statistically significant. In addition to its effect on Rel_p, intracellular Ca^{2+} also affects the maintained Rel. Fig. 7 *C* shows that, when the nominal $[Ca^{2+}]_i$ is 10 nM, the decay of the maintained phase in the Rel waveform has a faster time course than when the nominal $[Ca^{2+}]_i$ is 50 nM. Although the exact values of τ_2 have no significance, because ApIII was used (see discussion above), qualitative comparison of the values is still meaningful. This is consistent with the idea that the calcium store of the SR is probably less full when $[Ca^{2+}]_i$ is 10 nM than when it is 50 nM.

Site of action of external anions

Because the replacement of Cl^- with an impermeant anion happens outside a fiber, one wonders how the information is conveyed to the calcium release channels. One obvious possibility is a mediation through the voltage sensors. Unfortunately, in fibers containing 20 mM EGTA without added calcium, the anion substitution does not appear to have much effect on Q_γ but a replacement of Cl^- with SO_4^{2-}, $CH_3SO_3^-$, and gluconate increases, maintains, and decreases, respectively, the amount of Q_β. These anion effects on Q_β and lack of effects on Q_γ do not match the pattern of the effects on $Rel_{p,max}$ described above. However, this comparison might not be relevant, because under the conditions that the fibers can release Ca^{2+}, such as by reducing the $[EGTA]_i$ to 0.1 mM, the characteristics of Q_γ are drastically changed (Hui and Chen, 1997). Thus, the possible mechanism of the enhancement of calcium release by external Cl^- via the voltage sensors requires the support from an enhancement of charge movement by external Cl^- when the nominal $[Ca^{2+}]_i$ is 50 nM, and the evidence is not available yet. At present, it is very difficult to estimate the amount of Q_β and Q_γ from fibers containing 50 nM nominal $[Ca^{2+}]_i$ and being bathed in a Cl^- external solution because of the presence of the calcium-dependent Cl^- current. Hence, the enhancement via the voltage sensors remains an open possibility.

Alternatively, calcium release from the SR can be enhanced by the Cl^- present in the myoplasm. This idea arises from the observations that Cl^- greatly enhances calcium release through channels in lipid bilayers and SR vesicles (Sukhareva et al., 1994; Patel et al., 1996). Although the $[Cl^-]_i$ in live fibers is not expected to reach the same level as in lipid bilayer or SR vesicle experiments, a smaller $[Cl^-]_i$ might still be sufficient to bring forth an enhancing effect to the lesser extent reported in this paper. It is possible that the few millimolar Cl^- present in the myoplasm at rest is supplemented by Cl^- entered through Ca-independent and Ca-dependent Cl^- channels (Hui and Chen, 1994). One intervention that might be used to support the Cl^- entry hypothesis is to apply Cl^- channel blockers to investigate whether the enhancement is blocked. Another bonus offered by the blockade of Cl^- entry is that it might make the

analysis of Q_β and Q_γ in fibers containing normal $[Ca^{2+}]_i$ more straightforward (see preceding paragraph). Unfortunately, none of the blockers studied so far is as effective as the impermeant anions or high $[EGTA]_i$ in abolishing the calcium-dependent Cl^- current (Hui and Chen, 1994). It is hoped that a more ideal Cl^- channel blocker will be identified and the intervention will be tried in the future. The conclusion that can be drawn from the results will still have to rely on the assumption that the Cl^- channel blockers have no side effect on the voltage sensors.

Possible origins of the peak and maintained components of calcium release

The differential effects of replacing Cl^- with $CH_3SO_3^-$ on the amplitudes of the peak and the maintained phase of the Rel waveform (Fig. 8) might shed some light on the origin(s) of the two phases. As mentioned in the Introduction, the early peak and the maintained phase have been hypothesized to be two distinct components, the former being gated by Ca^{2+} and the latter by voltage. It is somewhat difficult to separate the Rel waveform into the two components because the shape of the rising phase of the maintained component is unknown. However, for the sake of discussion, if the amplitude of the calcium-gated component is taken as the difference between the amplitude of the peak and that of the maintained plateau, then its values are 16.7, 7.8, 1.7, and 6.9 $\mu M\ ms^{-1}$ in traces 1, 2, 4, and 5, respectively. This implies that a replacement of Cl^- with $CH_3SO_3^-$ has opposite and reversible effects on the two components; namely, it suppresses the calcium-gated component but enhances the voltage-gated component.

Although it is difficult to imagine how the anion substitution can exert opposite effects on the two components of Rel, one subtle point needs to be clarified. When Cl^- is used in the external solution, the space constant along the transverse tubular membrane is shorter than that when an impermeant anion is used. As a result, the depolarization during a test pulse is decremented from the surface toward the axis of the fiber to a greater extent when Cl^- is used. This, in turn, is expected to lead to a lower rate of calcium release averaged over the whole fiber cross-section. Hence, the observed enhancement of the maintained component, if it is voltage-gated, could be, in part, a consequence of the increase in space constant when an impermeant anion is used. To test this hypothesis, it is necessary to compare the potential profiles along the transverse tubules when different anions are used with the help of a potentiometric indicator and to correlate the difference in voltage decrements with the difference in the amplitudes of the maintained component quantitatively.

Alternatively, there could be simply one component of Rel and the decay of Rel from the peak to the maintained phase could be caused by calcium inactivation of the release. Following this view, the Rel was inactivated by 63% from the peak to the plateau in Cl^- (trace 1). After the $CH_3SO_3^-$ replacement, the inactivation was reduced to 37% when Rel_p was reduced (trace 2). The inactivation was progressively reduced to 17% when Rel_p was progressively reduced (trace 4). After washout, the inactivation was greatly restored to 55% when Rel_p was restored (trace 5). Thus, the degree of inactivation was qualitatively parallel to the magnitude of Rel_p.

This project was supported by a grant from the National Institutes of Health (NS21955).

REFERENCES

Armstrong, C. M., F. Bezanilla, and P. Horowicz. 1972. Twitches in the presence of ethylene glycol bis(β-aminoethyl ether)-N,N,N′,N′-tetraacetic acid. *Biochem. Biophys. Acta.* 267:605–608.

Baylor, S. M., W. K. Chandler, and M. W. Marshall. 1982a. Optical measurements of intracellular pH and magnesium in frog skeletal muscle fibres. *J. Physiol. (Lond.).* 331:105–137.

Baylor, S. M., W. K. Chandler, and M. W. Marshall 1982b. Use of metallochromic dyes to measure changes in myoplasmic calcium during activity in frog skeletal muscle fibres. *J. Physiol. (Lond.).* 331:139–177.

Baylor, S. M., W. K. Chandler, and M. W. Marshall. 1982c. Dichroic components of arsenazo III signals in skeletal muscle fibres. *J. Physiol. (Lond.).* 331:179–210.

Baylor, S. M., W. K. Chandler, and M. W. Marshall. 1983a. Sarcoplasmic reticulum calcium release in frog skeletal muscle fibres estimated from arsenazo III calcium transients. *J. Physiol. (Lond.).* 344:625–666.

Baylor, S. M., M. E. Quinta-Ferreira, and C. S. Hui. 1983b. Comparison of isotropic calcium signals from intact muscle fibers injected with arsenazo III or antipyrylazo III. *Biophys. J.* 44:107–112.

Chandler, W. K., and C. S. Hui. 1990. Membrane capacitance in frog cut twitch fibers mounted in a double Vaseline-gap chamber. *J. Gen. Physiol.* 96:225–256.

Colquhoun, D., and F. J. Sigworth. 1983. Fitting and statistical analysis of single-channel records. *In* Single-Channel Recording. B. Sakmann and E. Neher, eds. Plenum Press, New York. 191–263.

Endo, M., M. Tanaka, and Y. Ogawa. 1970. Calcium-induced release of calcium from the sarcoplasmic reticulum of skinned skeletal muscle fibres. *Nature.* 228:34–36.

Fabiato, A. 1985. Time and calcium dependence of activation and inactivation of calcium-induced release of calcium from the sarcoplasmic reticulum of a skinned canine cardiac Purkinje cell. *J. Gen. Physiol.* 85:247–289.

Ford, L. E., and R. J. Podolsky. 1970. Regenerative calcium release within muscle cells. *Science.* 167:58–59.

Hirota, A., W. K. Chandler, P. L. Southwick, and A. S. Waggoner. 1989. Calcium signals recorded from two new purpurate indicators inside frog cut twitch fibers. *J. Gen. Physiol.* 94:597–631.

Hollingworth, S., A. B. Harkins, N. Kurebayashi, M. Konishi, and S. M. Baylor. 1992. Excitation-contraction coupling in intact frog skeletal muscle fibers injected with mmolar concentrations of fura-2. *Biophys. J.* 63:224–234.

Huang, C. L.-H. 1982. Pharmacological separation of charge movement components in frog skeletal muscle. *J. Physiol. (Lond.).* 324:375–387.

Hui, C. S. 1983a. Pharmacological studies of charge movement in frog skeletal muscle. *J. Physiol. (Lond.).* 337:509–529.

Hui, C. S. 1983b. Differential properties of two charge components in frog skeletal muscle. *J. Physiol. (Lond.).* 337:531–552.

Hui, C. S. 1991. Factors affecting the appearance of the hump charge movement component in frog cut twitch fibers. *J. Gen. Physiol.* 98: 315–347.

Hui, C. S. 1997. Effect of external anion on calcium release in frog skeletal muscle fibers. *Biophys. J.* 72:A120.

Hui, C. S., and W. K. Chandler. 1990. Intramembranous charge movement in frog cut twitch fibers mounted in a double Vaseline-gap chamber. *J. Gen. Physiol.* 96:257–297.

Hui, C. S., and W. Chen. 1994. Origin of delayed outward ionic current in charge movement traces from frog skeletal muscle. *J. Physiol. (Lond.).* 479:109–125.

Hui, C. S., and W. Chen. 1995. Differential suppression of charge movement components by gluconate in cut twitch fibres of *Rana temporaria. J. Physiol. (Lond.).* 489:511–517.

Hui, C. S., and W. Chen. 1997. Charge movement in cut twitch fibres of *Rana temporaria* containing 0.1 mM EGTA. *J. Physiol. (Lond.).* 503: 563–570.

Irving, M., J. Maylie, N. L. Sizto, and W. K. Chandler. 1987. Intrinsic optical and passive electrical properties of cut frog twitch fibers. *J. Gen. Physiol.* 89:1–40.

Jacquemond, V., L. Csernoch, M. G. Klein, and M. F. Schneider. 1991. Voltage-gated and calcium-gated calcium release during depolarization of skeletal muscle fibers. *Biophys. J.* 60:867–873.

Jong, D.-S., P. C. Pape, W. K. Chandler, and S. M. Baylor. 1993. Reduction of calcium inactivation of sarcoplasmic reticulum calcium release by fura-2 in voltage-clamped cut twitch fibers from frog muscle. *J. Gen. Physiol.* 102:333–370.

Jong, D.-S., P. C. Pape, S. M. Baylor, and W. K. Chandler. 1995. Calcium inactivation of calcium release in frog cut muscle fibers that contain millimolar EGTA or fura-2. *J. Gen. Physiol.* 106:337–388.

Klein, M. G., B. J. Simon, and M. F. Schneider. 1990. Effects of caffeine on calcium release from the sarcoplasmic reticulum in frog skeletal muscle fibres. *J. Physiol. (Lond.).* 425:599–626.

Klein, M. G., B. J. Simon, and M. F. Schneider. 1992. Effects of procaine and caffeine on calcium release from the sarcoplasmic reticulum in frog skeletal muscle. *J. Physiol. (Lond.).* 453:341–366.

Konishi, M., and S. M. Baylor. 1991. Myoplasmic calcium transients monitored with purpurate indicator dyes injected into intact frog skeletal muscle fibers. *J. Gen. Physiol.* 97:245–270.

Kovacs, L. E., E. Rios, and M. F. Schneider. 1979. Calcium transients and intramembrane charge movement in skeletal muscle fibres. *Nature.* 279:391–396.

Kovacs, L. E., E. Rios, and M. F. Schneider. 1983. Measurement and modification of free calcium transients in frog skeletal muscle fibres by a metallochromic indicator dye. *J. Physiol. (Lond.).* 343:161–196.

Maylie, J., and C. S. Hui. 1991. Action of 2,3-butanedione monoxime on calcium signals in frog cut twitch fibres containing antipyrylazo III. *J. Physiol. (Lond.).* 442:551–567.

Maylie, J., M. Irving, N. L. Sizto, and W. K. Chandler. 1987a. Comparison of arsenazo III optical signals in intact and cut frog twitch fibers. *J. Gen. Physiol.* 89:41–81.

Maylie, J., M. Irving, N. L. Sizto, and W. K. Chandler. 1987b. Calcium signals recorded from cut frog twitch fibers containing antipyrylazo III. *J. Gen. Physiol.* 89:83–143.

Maylie, J., M. Irving, N. L. Sizto, G. Boyarsky, and W. K. Chandler. 1987c. Calcium signals recorded from cut frog twitch fibers containing tetramethylmurexide. *J. Gen. Physiol.* 89:145–176.

Melzer, W., M. F. Schneider, B. J. Simon, and G. Szucs. 1986. Intramembrane charge movement and calcium release in frog skeletal muscle. *J. Physiol. (Lond.).* 373:481–511.

Miledi, R., I. Parker, and G. Schalow. 1977. Measurement of calcium transients in frog muscle by the use of arsenazo III. *Proc. R. Soc. Lond. B Biol. Sci.* 198:201–210.

Palade, P., and J. Vergara. 1982. Arsenazo III and antipyrylazo III calcium transients in single skeletal muscle fibers. *J. Gen. Physiol.* 79:679–707.

Pape, P. C., D.-S. Jong, and W. K. Chandler. 1995. Calcium release and its voltage dependence in frog cut muscle fibers equilibrated with 20 mM EGTA. *J. Gen. Physiol.* 106:259–336.

Pape, P. C., D.-S. Jong, and W. K. Chandler. 1998. Effects of partial sarcoplasmic reticulum calcium depletion on calcium release in frog cut muscle fibers equilibrated with 20 mM EGTA. *J. Gen. Physiol.* 112: 263–295.

Patel, J. R., M. Sukhareva, R. Coronado, and R. Moss. 1996. Chloride-induced Ca^{2+} release from the sarcoplasmic reticulum of chemically skinned rabbit psoas fibers and isolated vesicles of terminal cisternae. *J. Membr. Biol.* 154:81–89.

Rios, E., and G. Pizarro. 1995. A calcium synapse model of control of Ca release in skeletal muscle. *Biophys. J.* 68:A175.

Schneider, M. F., and B. J. Simon. 1988. Inactivation of calcium release from the sarcoplasmic reticulum in frog skeletal muscle. *J. Physiol. (Lond.).* 405:727–745.

Schneider, M. F., B. J. Simon, and G. Szucs. 1987. Depletion of calcium from the sarcoplasmic reticulum during calcium release in frog skeletal muscle. *J. Physiol. (Lond.).* 392:167–192.

Simon, B. J., M. G. Klein, and M. F. Schneider. 1991. Calcium dependence of inactivation of calcium release from the sarcoplasmic reticulum in skeletal muscle fibers. *J. Gen. Physiol.* 97:437–471.

Sukhareva, M., J. Morrissette, and R. Coronado. 1994. Mechanism of chloride-dependent release of Ca^{2+} in the sarcoplasmic reticulum of rabbit skeletal muscle. *Biophys. J.* 67:751–765.

Vergara, J., and C. Caputo. 1983. Effects of tetracaine on charge movements and calcium signals in frog skeletal muscle fibers. *Proc. Natl. Acad. Sci. USA.* 80:1477–1481.